

Fabrication and Characterization of Novel Biphasic Calcium Phosphate and Nanosized Hydroxyapatite Derived from Fish Otoliths in Different Composition Ratios

Nerly D. Montañez*^a, Hugo A. Estupiñan^b, Sandra J. García^a, Darío Y. Peña^a

^aUniversidad Industrial de Santander, Carrera 27, Calle 9 Ciudad Universitaria Bucaramanga, Colombia.

^bUniversidad Nacional de Colombia, Facultad de Minas, sede Medellín, Antioquia, Colombia.

ing.nerly.montanez@hotmail.com

Biphasic calcium phosphate (BCP) is a ceramic material that can promote bone regeneration. However, there are controversies about the proportions of the phases in which the BCP must be combined in order to maintain their biological activity. In this study, a novel biphasic calcium phosphate from fish otoliths containing mixed phases of hydroxyapatite/ β -tricalcium phosphate (HA/ β -TCP) was fabricated by aqueous precipitation technique. Three compositions of BCP and three compositions of hydroxyapatite (HA) from otoliths of teleost fish (*Plagioscion squamosissimus*) were studied. X-ray diffraction analysis revealed that, at low pH values, multiphase calcium phosphate compounds were formed, whereas at high pH values single-phase hydroxyapatite was formed after 96 h of precipitation time. SEM micrographs showed agglomeration of particles with porous structures, as well as the presence of nanosized particles. The different vibration modes of the PO_4^{3-} ion was identified by Raman spectroscopy and FTIR.

1. Introduction

Biphasic calcium phosphate (BCP), composed of hydroxyapatite (HA) and β -tricalcium phosphate (β -TCP), has been used as scaffold for bone regeneration. The biodegradability and bioactivity of these materials have been widely evidenced. However, both phosphates exhibit different biological resorption capacities, so that an adequate balance between HA and β -TCP determine the mechanical properties, biodegradability and stability of the final phases (Shim et al., 2017 and Marques et al., 2017). The physicochemical properties of BCP, which are given by the synthesis process, facilitate cell attachment, proliferation and differentiation (Garrido et al., 2011). One of the main constituents of BCP is hydroxyapatite, which is the major mineral component of bones and teeth. It has been established that nanosized hydroxyapatite increases the bioactivity of biomaterials. Many routes for the synthesis of these calcium phosphates have been studied (Shojai et al., 2013). The use of precursors is limited to their solubility in water and the reagent cost (Medvecky et al., 2011). The raw material proposed in the present work has not been widely studied for this type of synthesis. The objective of this study was to evaluate the physicochemical characteristics of a biphasic calcium phosphate and nanosized hydroxyapatite synthesized from a bioceramic extracted from the inner ear cavity of fish (*Plagioscion squamosissimus* specie). An initial evaluation of the bioceramic, which has been previously reported, showed a biomineral structure composed of 82.5% aragonite and 17.5% amorphous (Montañez et al., 2017). The calcium phosphate obtained in different composition ratios is a novel material that can be used for bone regeneration.

2. Methodology

The bioceramic obtained from fish was washed with ethanol and deionized water in an ultrasonic bath for 1 h to remove impurities and then dried at room temperature. The otoliths were milled in a ball mill (Retsch PM 1000, 6 min, 5000 rpm, 10 s interval) and calcined at 1000 °C for 2 h. The otoliths powder was combined with 0.6 M orthophosphoric acid solution at 90 °C. To compare the pH and precipitation time conditions, the

solution was precipitated for 48 h at room temperature using pH values of 4, 5 and 6. The solution was also precipitated for 96 h at room temperature using pH values of 6, 8 and 10. The filtrate was oven-dried at 105°C for 24 h, then calcined at 1050°C for 3 h using a heating ramp of 2°C/min.

Chemical and morphological characterization was carried out by X-ray diffraction (XRD) using a Bruker D8 equipment. Fourier Transform Infrared Spectroscopy (FTIR) was conducted employing a Nicolet iS50 Spectrometer (4000 to 400 cm⁻¹). Raman spectroscopy was performed on a Labram HR Evolution HORIBA Scientific with a 532 nm laser, while scanning electron microscopy (SEM) was carried out using a FEI Quanta 650 FEG equipment, using secondary electrons image with a 8.5 mm working distance and acceleration voltage of 20 kV. The qualitative analysis of the phases present in the calcium phosphates was performed by comparing the profile observed with the diffraction profiles reported in the PDF-2 database of the International Center for Diffraction Data ICDD. The quantitative analysis of the phases was performed by refinement using the Rietveld method, adding a known internal standard quantity (Aluminum oxide, -100 mesh, 99%, Corundum, α -phase. Aldrich No. 23474-5) corresponding to 21.69, 21.52, 20.93, 20.61, 21.35 y 19.60 % for samples synthesized at pH 4, 5, 6 (48 h) and pH 6, 8 and 10 (96 h).

3. Results and discussion

XRD examination of the calcium phosphate synthesized at low pH showed the main characteristic peaks of HA at 2θ diffraction angles (25.8°, 31.7°, 32.2°, 32.8°, 34.1°, 46.9° and 49.4°), and main peaks for β -TCP (25.8°, 26.5°, 29.6°, 32.8° and 34.3°) (Ebrahimi et al., 2017a). The diffraction pattern agreed with the diffraction profiles reported in the PDF-2 ICDD PDF 010-76-0694 for hydroxyapatite and PDF 000-55-0898 for β -TCP (Figure 1(a)).

For the samples synthesized under high pH values, XRD shows peaks with significant intensity at 25.8°, 31.7-35°, 39.8°, 47-48°, 49.5° and 53.2°, indicating that the synthesized calcium phosphate has a crystalline hydroxyapatite phase (PDF 010-76-0694 of ICDD) (Figure 1(b)). The high intensity peaks at 30-35° suggested the presence of a crystalline phase of nanosized hydroxyapatite (Poinern et al., 2009 and Matthews et al., 2016).

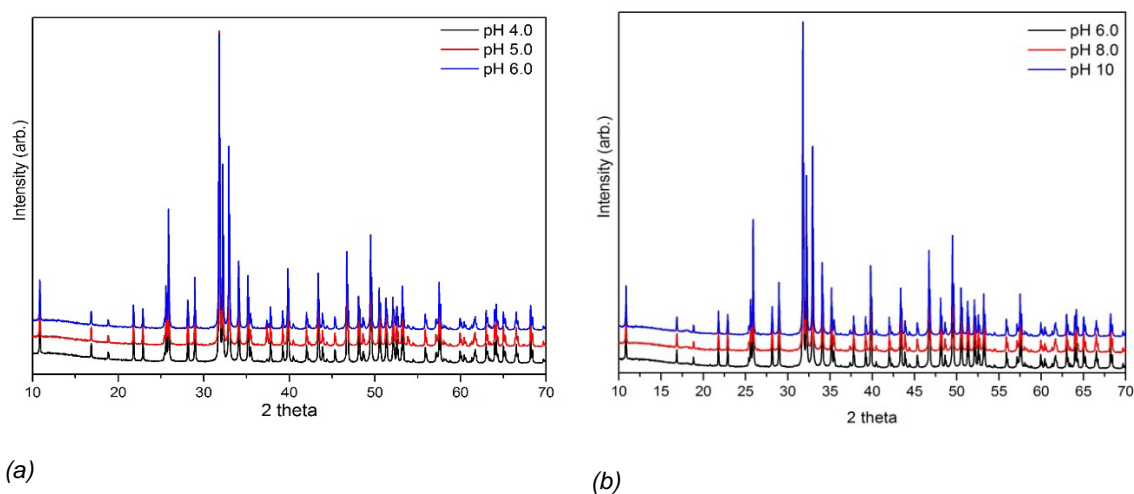


Figure 1: X-ray diffraction patterns of the synthesized calcium phosphate at (a) pH values of 4, 5 and 6 and (b) pH values of 6, 8 and 10.

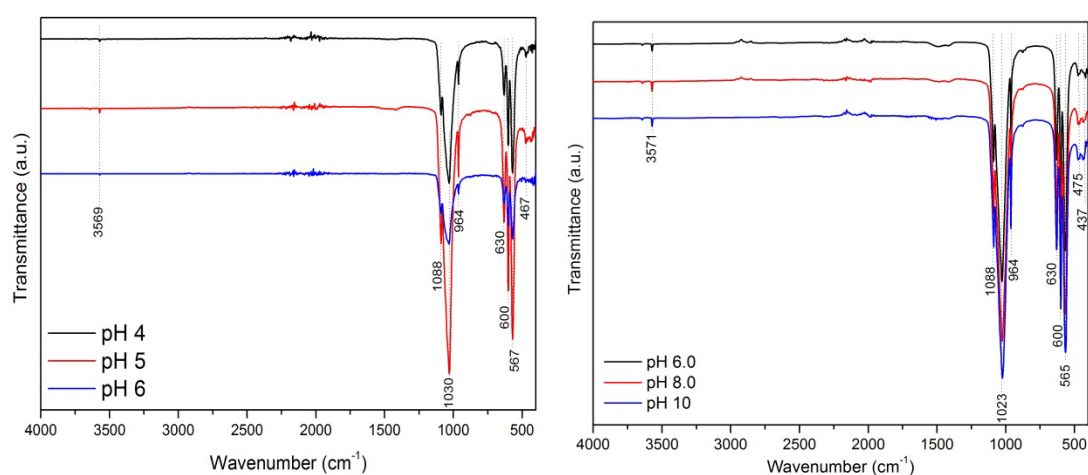
The quantitative percentages from the Rietveld analysis are shown in Table 1. Regardless of the pH values used in the synthesis, it was possible to quantify the amount of hydroxyapatite. Although the β -TCP phase was identified, there was no model in the database to perform its corresponding quantification. For higher precipitation times, as the pH increased, the amount of crystalline hydroxyapatite increased, and therefore the amount of total amorphous phases decreased. Moreover, for lower precipitation times, the percentage of crystalline hydroxyapatite phase did not appear to show a trend, although the total amount of amorphous decreased compared to the 96h samples. Other secondary phases were found (Calcium oxide (CaO)), which was probably due to phase decomposition or transformation during processing (such as sintering) (Ebrahimi et al., 2017b).

Table 1: Rietveld analysis of the methods for synthesis of calcium phosphates at pH values of 4, 5, 6 (48h) and pH values of 6, 8 and 10 (96h).

pH	Precipitation time (h)	Hydroxyapatite	β -TCP	CaO	Total Amorphous
4.0	48	89.0 %	NQ*	0.4 %	10.6 %
5.0	48	78.3 %	NQ	2.4 %	19.3 %
6.0	48	82.2 %	NQ	1.1 %	16.7 %
6.0	96	75.6 %	-	0.5 %	23.9 %
8.0	96	78.1 %	-	0.5 %	21.4 %
10.0	96	80.4 %	-	0.6 %	19.0 %

*NQ: Not Quantifiable

FTIR analysis reveals that the synthesized calcium phosphate shows absorption bands corresponding to ion PO_4^{3-} around 1088 cm^{-1} (ν_3), $1023\text{-}1030\text{ cm}^{-1}$ (ν_3), 964 cm^{-1} (ν_1), 600 cm^{-1} (ν_4), $565\text{-}567\text{ cm}^{-1}$ (ν_4) and $467\text{-}475\text{ cm}^{-1}$ assigned to bending O-P-O (ν_2) (Figure 2). There are also absorption bands corresponding to OH-around 3570 cm^{-1} and 630 cm^{-1} (deformation P-OH vibration), indicating that the synthesized calcium phosphate contains significant amounts of HA. The observed bands have been attributed to β -TCP and HA powders (Poinern et al., 2009, Dalmónico et al., 2015 and Marques et al., 2017).



(b)

Figure 2: FTIR spectra of synthesized calcium phosphate at (a) pH values of 4, 5 and 6 and (b) pH values of 6, 8 and 10.

The typical Raman band assignments for bone are $422\text{-}454\text{ cm}^{-1}$ corresponding to PO_4^{3-} (ν_2), $568\text{-}617\text{ cm}^{-1}$ corresponding to PO_4^{3-} (ν_4), $957\text{-}962\text{ cm}^{-1}$ corresponding to PO_4^{3-} (ν_1), $1006\text{-}1055\text{ cm}^{-1}$ corresponding to PO_4^{3-} (ν_3) and $3572\text{-}3575\text{ cm}^{-1}$ corresponding to OH stretching (Khan et al., 2013). The peaks in the spectrums presented in Figures 3 and 4 are consistent with the previously described bands. The slight changes in the peaks are due to changes in the crystallinity of the samples, which was caused by variation of the synthesis parameters.

For β -TCP, a peak around 549 cm^{-1} decreased for temperatures greater than $1000\text{ }^\circ\text{C}$ (Kim et al., 2014), which explains the identification of the β -TCP phase by XRD, although it was not clearly observed in the Raman spectrum. The peak at $\sim 583\text{ cm}^{-1}$ is attributed to the HA phase for PO_4^{3-} (ν_4), also found in Figure 4. The peaks at 955 cm^{-1} and 969 cm^{-1} in Figures 3 and 4, respectively, suggest the significant presence of the HA phase (Gao et al., 2013).

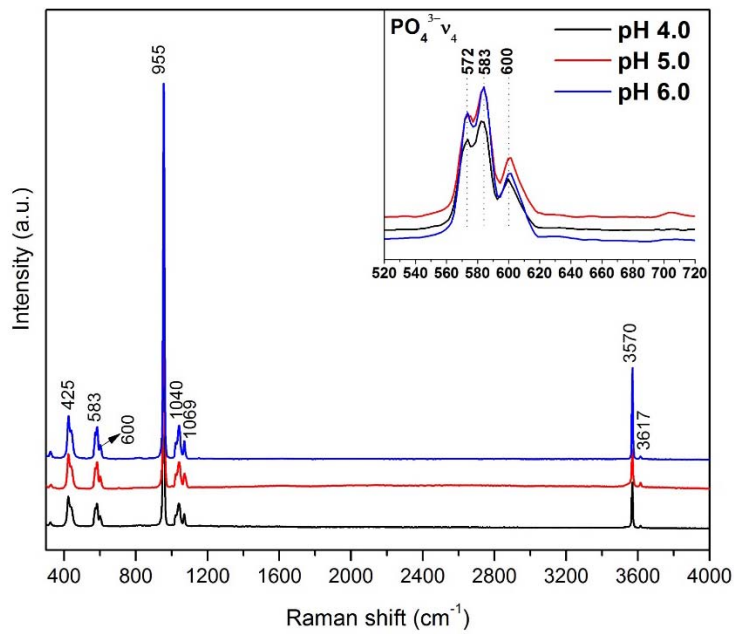


Figure 3: Raman spectrum for synthesized calcium phosphate at pH values of 4, 5 and 6, for 48 h.

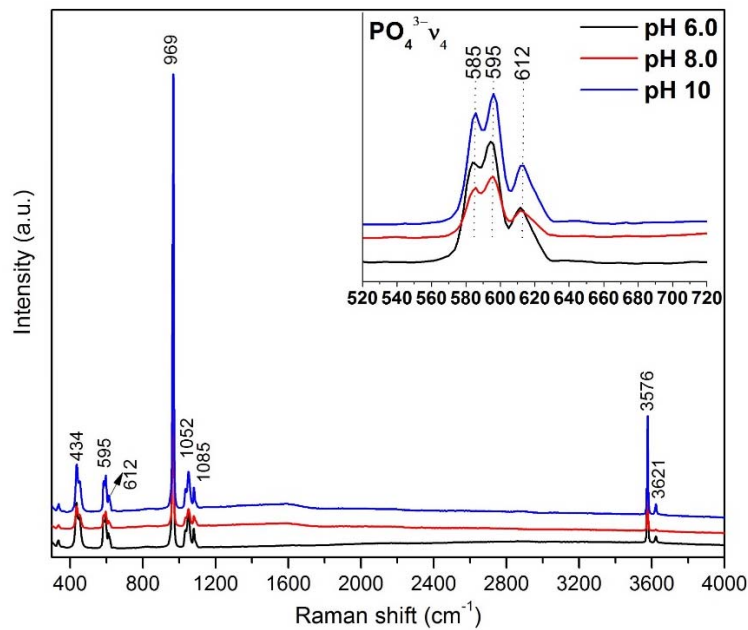


Figure 4: Raman spectrum for synthesized calcium phosphate at pH values of 6, 8 and 10, for 96 h.

Figure 5 shows scanning electron micrographs of nanosized calcium phosphate particles synthesized at pH between 4 and 10. The morphology is very similar between the samples synthesized at different precipitation times. However, at high pH and precipitation time (96 h), the particle size decreases. Calcium phosphates densified with spheroidal shape and micro-pores, being the sample treated at pH 6 for 48 h (Figure 5 (c)) the most densified. Apart from the chemistry of the material, densification and porosity affect the biocompatibility of the material, which will be investigated in future work.

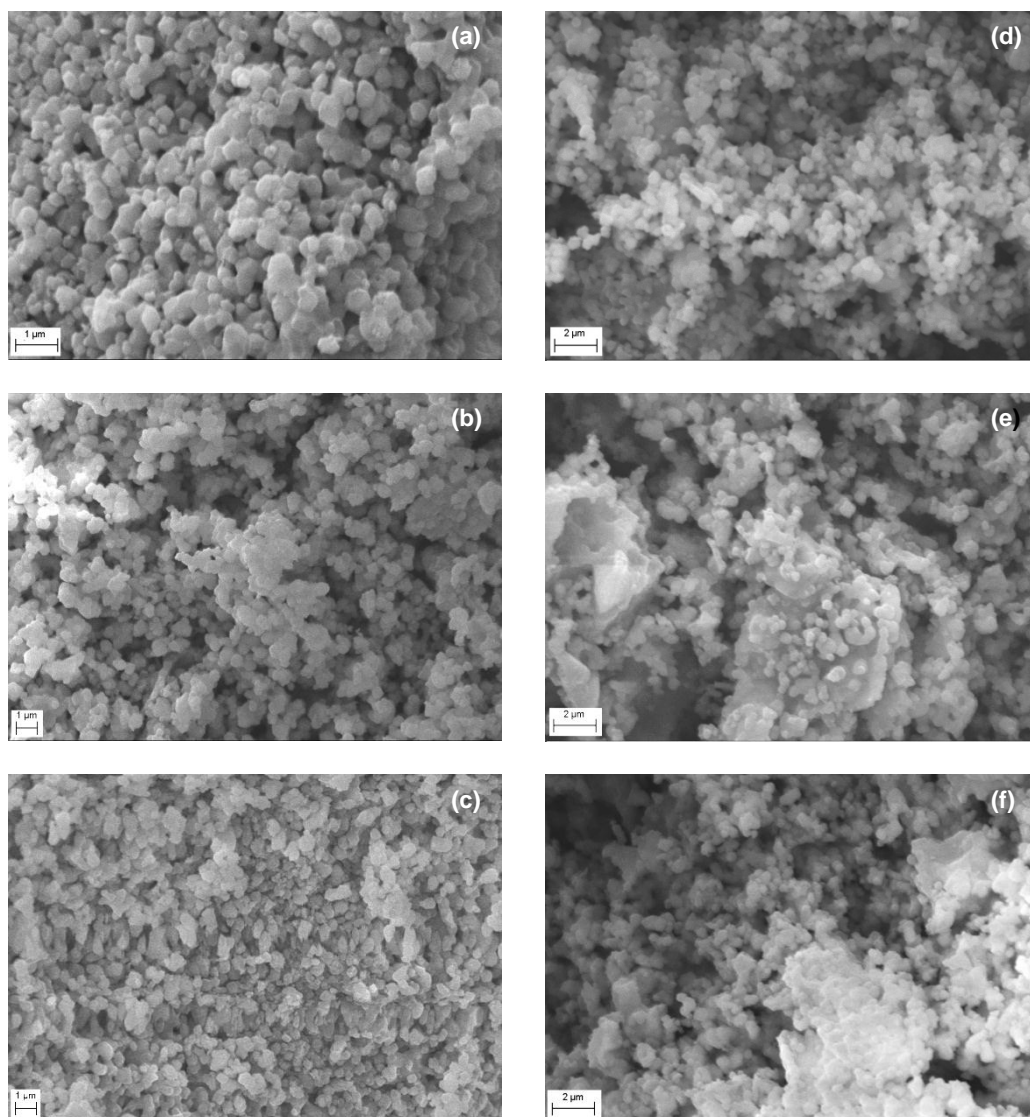


Figure 5: SEM micrographs of calcium phosphate synthesized for 48 h at (a) pH 4, (b) pH 5 and (c) pH 6. For 96 h at (d) pH 6, (e) pH 8, and (f) pH 10.

4. Conclusions

The synthesis of BCP and nanosized hydroxyapatite was performed using the precipitation method and otoliths from fish as raw material. The percentage of crystallinity is considerable and it is independent of the time of synthesis and the pH value used. It is clear that the concentration of the species involved in the process of synthesis has a more significant effect on the crystallinity of the resulting material, relative to the pH and precipitation times used. The physicochemical properties of the synthesized calcium phosphates are suitable for their use as biomaterials, which makes otoliths a novel material for bone regeneration.

Acknowledgments

The authors are grateful to Jaimes Rueda & Cia Ltda, Universidad Industrial de Santander, Vicerrectoría de Investigación y Extension and Grupo de Investigaciones en Corrosión for support of this work (Internal project code 1888).

References

Dalmónico G., Silva D., Franczar P., Camargo N., Rodríguez M., 2015, Elaboration biphasic calcium phosphate nanostructured powders, *Boletín de la Sociedad Española de Cerámica y Vidrio*, 54, 37-43.

- Ebrahimi M., Botelho M., 2017a, Biphasic calcium phosphates (BCP) of hydroxyapatite (HA) and tricalcium phosphate (TCP) as bone substitutes: Importance of physicochemical characterizations in biomaterials studies, *Data in Brief*, 10, 93-97.
- Ebrahimi M., Botelho M., Dorozhkin S., 2017b, Biphasic Calcium Phosphates bioceramics (HA/TCP): Concept, physicochemical properties and the impact of standardization of study protocols in biomaterials research, *Material Science and Engineering C*, 71, 1293-1312.
- Garrido C., Lobo S., Turfio F., LeGeros R., 2011, Biphasic calcium phosphate bioceramics for orthopaedic reconstructions: Clinical outcomes, *International Journal of Biomaterials*, 2011, 1-9.
- Gao C., Yang B., Hu H., Liu J., Shuai C., Peng S., 2013, Enhanced sintering ability of biphasic calcium phosphate by polymers used for bone scaffold fabrication, *Material Science and Engineering C*, 33, 3802-3810.
- Khan A-F., Awais M., Khan A-S., Tabassum S., Chaudhry A., Rehman I., 2013, Raman Spectroscopy of Natural Bone and Synthetic Apatites, *Applied Spectroscopy Reviews*, 48, 329-355.
- Kim D., Chun H., Lee J., Yoon S., 2014, Evaluation of phase transformation behaviour in biphasic calcium phosphate with controlled spherical micro-granule architecture, *Ceramics International*, 40, 5145-5155.
- Marques C., Olhero S., Abrantes J., Marote A., Ferreira S., Vieira S., Ferreira J., 2017, Biocompatibility and antimicrobial activity of biphasic calcium phosphate powders doped with metal ions for regenerative medicine, *Ceramics International*, 43, 15719-15728.
- Mattews M., Khalid M., Ratnam C., Chee C., Rashmi W., Hoque M., 2016, Sono-synthesis of nanohydroxyapatite: Effects of process parameters, *Ceramics International*, 42, 6263-6272.
- Medvecky L., Sopcak T., Durisin J., Briancin J., 2011, Nanohydroxyapatite prepared from non-toxic organic Ca²⁺ compounds by precipitation in aqueous solution, *Materials Letters*, 65, 3566-3569.
- Montañez N., Sandoval A., Estupiñan H., Peña D., 2017, A novel biphasic calcium phosphate derived from fish otoliths, *Journal of Physics: Conference Series*, 935, 012037.
- Poinern G., Brundavanam R., Mondinos N., Jiang Z., 2009, Synthesis and characterization of nanohydroxyapatite using an ultrasound assisted method, *Ultrasonics Sonochemistry*, 16, 469-474.
- Shim K., Kim S., Yun Y., Jeon D., Kim H., Park K., Song H., 2017, Surface Immobilization of biphasic calcium phosphate nanoparticles on 3D printed poly(caprolactone) scaffolds enhances osteogenesis and bone tissue regeneration, *Journal of Industrial and Engineering Chemistry*, 55, 101-109.
- Shojai M., Mohammad K., Ehsan D., Jamshidi A., 2013, Synthesis methods for nanosized hydroxyapatite with diverse structures, *Acta Biomaterialia*, 9, 7591-7621.